ARTICLE NO. 78-978R

Erosive Burning Study of Composite Solid Propellants by Turbulent Boundary-Layer Approach

M. K. Razdan* and K. K. Kuo†
The Pennsylvania State University, University Park, Pa.

Erosive burning of composite solid propellants is investigated by analyzing a steady, two-dimensional, chemically reacting, turbulent boundary layer over a propellant surface. Predicted erosive burning rates agree closely with experimental data. The erosive burning rate augmentation is found to be caused by the increase in heat feedback introduced by the increase in transport coefficients, and the turbulence enhanced mixing and reaction of the oxidizer and fuel gases. The increase in freestream gas velocity brings the location of the peak turbulence intensity and the heat release zone closer to the propellant surface, thereby increasing the burning rate of a propellant.

Nomenclature

a = reaction time parameter in Summerfield's burning rate law, psia/in./s
A_g = Arrhenius frequency factor in gaseous reactions, $(m^3)^{n-1}s^{-1}$ (kmole)$^{1-n}$
A_s = Arrhenius frequency factor in propellant surface decomposition, m/s
A^+ = damping constant in van Driest's hypothesis
b = diffusion time parameter in Summerfield's burning rate law, psia$^{1/3}$/in./s
$C_1 \rightarrow C_4, C_\mu, C_\rho, C_\omega$ = constants in turbulence models
C_p $\equiv \Sigma_k Y_k C_{pk}$, average heat capacity of the reacting gases, kcal/kg-K
C_{pk} = heat capacity of the kth species, kcal/kg-K
C_s = heat capacity of solid propellant, kcal/kg-K
D = diffusion coefficient in Fick's Law, m^2/s
$\mathfrak{D}$ = damping coefficient defined in Eq. (26)
E_{ag}, E_{as} = activation energies in the gas phase reaction and propellant surface decomposition, kcal/mole
g_F $\equiv \overline{Y'^2_F}$, mean square of fuel mass-fraction fluctuations
$\Delta h^\circ_{f,k}$ = heat of formation of the kth species, kcal/kg
h_k $\equiv \Delta h^\circ_{f,k} + \int_{T^\circ}^{T} C_{pk} dT$, static enthalpy of the kth species, kcal/kg
H $\equiv \Sigma_k Y_k h_k + u_i u_i/2$, stagnation enthalpy of gases, kcal/kg
k = Von Karman's constant
K $\equiv \overline{u'_i u'_i}/2$, turbulent kinetic energy, m^2/s^2
n = order of chemical reaction
p = pressure, N/m^2
Pr $\equiv C_p \mu/\lambda$, Prandtl number based upon the molecular properties of the fluid
Pr_t = Prandtl number for turbulent flow defined in Eq. (8)
$\dot{Q}_r$ $\equiv \Sigma_k (\nu_k W_k \Delta h^\circ_{f,k} \bar{\omega}_k)/(\nu_F W_F)$, rate of heat generation in gas phase, kcal/m^3-s
Q_s = heat of reaction defined in Eq. (22), kcal/kg
r_b = total burning rate of a solid propellant, m/s
r_{b0} = strand burning rate of a solid propellant, m/s
Re_x $\equiv \rho_\infty U_\infty x/\mu_\infty$, Reynolds number based on x
R_h = roughness height, m
R_u = universal gas constant, N-m/kmole-K
Sc $\equiv \mu/\bar{\rho}D$, Schmidt number based upon molecular properties of the fluid
Sc_t = Schmidt number for turbulent flow defined in Eq. (8)
T = temperature, K
T° = reference temperature, 298.14 K
T_p = propellant temperature, K
T_{pi} = propellant initial temperature, K
T_{ps} = propellant surface temperature, K
$\bar{T}_{ps}$ = reference surface temperature of the propellant, K
u = gas velocity in x direction, m/s
U_∞ = freestream velocity, m/s
u_* $\equiv \sqrt{\tau_w/\rho_\infty}$, friction velocity, m/s
v = gas velocity in y direction, m/s
W $\equiv (\Sigma_k Y_k/W_k)^{-1}$, average molecular weight of gases, kg/kmole
W_k = molecular weight of the kth species, kg/kmole
x = coordinate along the propellant surface, m
y = coordinate normal to the propellant surface, m
Y_k = mass fraction of the kth species
Y_{FS} = mass fraction of fuel in a composite solid propellant
Y_{OS} = mass fraction of oxidizer in a composite solid propellant

Presented as Paper 78-978 at the AIAA/SAE 14th Joint Propulsion Conference, Las Vegas, Nev., July 25-27, 1978; submitted Oct. 6, 1978; revision received May 18, 1979.

Index categories: Solid and Hybrid Rocket Engines; Reactive Flows; Boundary Layers and Convective Heat Transfer—Turbulent.

*Assistant Professor, Dept. of Mechanical Engineering. Member AIAA.
†Associate Professor, Dept. of Mechanical Engineering. Member AIAA.

$\overline{()}$ = time-averaged quantity
$()'$ = fluctuating quantity
$()_{,i}$ = partial differentiation of the quantity in $()$ with respect to x_i, $()/m$
δ = boundary-layer thickness, m
ϵ $\equiv \mu \overline{u'_{i,j} u'_{i,j}}/\bar{\rho}$, turbulent dissipation, m^2/s^3
λ = thermal conductivity of the gas, kcal/m-s-K
λ_s = thermal conductivity of the solid propellant, kcal/m-s-K
μ = gas viscosity, kg/m-s
μ_{eff} $\equiv \mu + \mu_t$, effective viscosity, kg/m-s
μ_t = turbulent viscosity defined in Eq. (11), kg/m-s
$(\mu/Pr)_{\text{eff}}$ $\equiv (\mu/Pr) + (\mu_t/Pr_t)$, kg/m-s
$(\mu/Sc)_{\text{eff}}$ $\equiv (\mu/Sc) + (\mu_t/Sc_t)$, kg/m-s
ν_k = number of kmoles of the kth species
ρ = gas density, kg/m^3
ρ_s = solid propellant density, kg/m^3
τ $\equiv \mu_{\text{eff}} \partial \bar{u}/\partial y$, local shear stress, N/m^2
$\dot{\omega}_k$ = rate of production of species k due to chemical reactions, kg/m^3-s

Subscripts

k = species index representing fuel gas $[F]$, oxidizer gas $[O]$, and product gas $[P]$
∞ = freestream condition
w = wall (propellant surface) condition

I. Introduction

EROSIVE burning is a common phenomenon experienced in solid-propellant rocket motors, and generally represents an increase in propellant burning rate due to high-velocity combustion gases flowing parallel to the propellant surface. The ability to predict the burning rate is of prime importance in the design of a rocket motor, because both the thrust level and the burning time depend on the burning rate. Erosive burning is a serious problem in high-performance rockets and missiles with high-thrust, short-burning, solid-propellant motors. Nozzleless rocket motors recently have attracted considerable interest because they offer significant economic advantage over more conventional motors. Nozzleless rocket motors have low port-to-throat area ratios in which the gas velocity reaches sonic and supersonic speeds over the propellant surfaces, leading to the extremely serious problem of erosive burning.

In the past, the problem of erosive burning has been investigated by various methods, as reported in literature reviews by Kuo and Razdan,[1] and King.[2] Existing theories on erosive burning, in general, can be divided into three distinct classes, depending upon whether the theory is based on 1) a phenomenological heat-transfer theory that does not take into account chemical reactions and/or flame structure, 2) a flame theory based on a description of combustion mechanisms and/or flame structure, or 3) an aerothermochemical analysis that includes the consideration of heat, mass, and momentum transfer in a chemically reacting boundary layer.

Among phenomenological heat-transfer theories, the Lenoir-Robillard theory[3] is referred to most often. The essence of this theory is that erosive burning rate is proportional to the forced convective heat-transfer coefficient. Representative work on erosive burning based on flame theory has been reported by Vandenkerckhove,[4] who considered the flame structure and the mechanism of solid phase decomposition in a double-based solid propellant. King[5] has developed a model for the erosive burning of composite propellant, based on the assumption that the crossflow of gases bends the diffusion flame, thus bringing the heat release zone closer to the propellant surface.

The erosive burning theory based on the boundary-layer approach was first reported in the early work of Corner,[6] who used the Prandtl-Karman boundary-layer theory to describe the flowfield. Tsuji,[7] Razdan,[8] and Schuyler and Torda[9] analyzed the problem by considering a laminar boundary layer over the propellant surface. However, it must be noted that the flow in an erosive burning situation is normally turbulent. Lengelle[10] used the integral solutions of turbulent boundary-layer equations in combination with a diffusion flame theory to develop his model. Beddini[11] has used a multiequation turbulence closure model to solve the boundary-layer problem. He considered the combustion of hemogeneous propellants.

Although there are differing emphases in various approaches to solving the problem of erosive burning, the most realistic analysis must consider the interaction between flame zone structure and the flowfield. In this paper, such an interaction is considered through an aerothermochemical analysis of the problem, which includes the consideration of heat, mass, and momentum transfer in a chemically reacting turbulent boundary layer. The development of the current model is based on the combustion of the most commonly used ammonium perchlorate (AP) composite propellants and is, therefore, limited to these types of heterogeneous propellants.

Most of the successful strand-burning models[12,13] of composite solid propellants consider the dominant effect of oxidizer-fuel (O/F) diffusion flame on the burning rate of the propellant. At normal rocket pressures (in the order of 100 atm), the pressure dependence of the burning rate of a composite propellant, as pointed out by Steinz et al.,[12] is brought about through the diffusion flame. Steinz et al. also note that the scale of unmixedness, as it affects the diffusion flame, is an important aspect of the burning process. In the presence of a flowfield, it is this diffusion flame that interacts with the turbulent crossflow of gases and, therefore, affects the heat flux to the propellant surface and the burning rate. Figure 1 clearly illustrates this point. The plot is based on the experimental data of Refs. 5 and 14. The erosive-burning data for various freestream velocities was taken from King's work.[5] With known blowing rates and freestream velocities, the corresponding friction coefficient was obtained from Simpson and MacQuaid's data reported in Ref. 14. The data on friction coefficient are also available from earlier work by Mickley and Davis.[15] However, the crossflow velocities in their work were quite low (about 18 m/s) and their data are correlated with (v_w/U_∞), rather than the conventional mass blowing parameter $(\rho v)_w/(\rho U)_\infty$. Figure 1 shows that the domain of turbulence is very close to the propellant surface and that it interacts with the diffusional reaction zone, which is about 20-100 μm from the propellant surface. Makunda's[16] calculations also show that the flame zone is in the turbulence region of the flowfield. With increasing crossflow velocities, the domain of turbulence comes closer to the propellant surface (see Fig. 1). It is clear that the diffusion flame is in a region where the turbulence cannot be ignored.

The objectives of the present study are: 1) to formulate a theoretical model, based on an aerothermochemical analysis of the erosive burning problem of composite solid propellants, which considers the heat, mass, and momentum transfer in a chemically reacting turbulent boundary layer; 2) to solve the theoretical model and to study the effects of gas velocity, pressure, and propellant physicochemical characteristics on the erosive burning rate of a composite solid propellant; and 3) to test the validity of the theoretical model by comparing the predicted erosive burning rates with experimental data.

II. Analysis

A. Description of the Physical Model

The physical model considered in the theoretical analysis consists of a flat plate with a fixed leading edge as shown in Fig. 2. A two-dimensional propellant slab glued to the

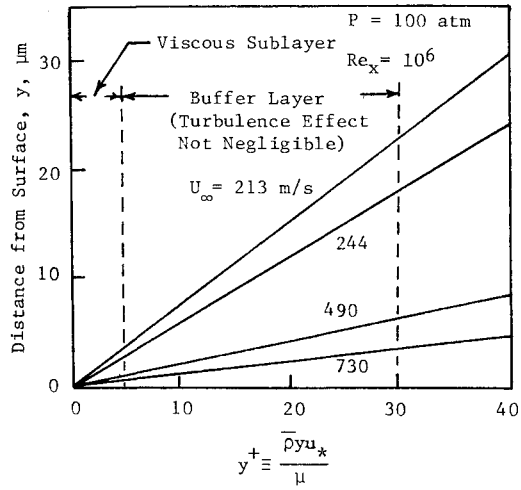

Fig. 1 Effect of freestream velocity on the domain of turbulence near a propellant surface.

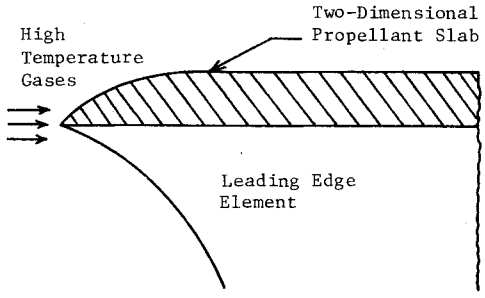

Fig. 2 Physical model considered in the theoretical formulation.

leading-edge element is ignited by the hot combustion gas in the freestream, which forms a turbulent boundary layer over the burning surface of the propellant. The boundary layer is considered to be quasisteady, two-dimensional, and chemically reacting.

B. Conservation Equations

To formulate the theoretical model, one begins with the general conservation equations for a reacting compressible fluid flow. In these equations, each instantaneous variable is replaced by its mean and fluctuating part (this is the well-known Reynolds' decomposition procedure), and all equations are time averaged.[17] The following assumptions are then introduced into these equations: 1) the averaged flow properties are steady; 2) the mean flow is two dimensional; 3) for a flow of Mach number of order one,

$$\overline{\mu'(\partial u'/\partial y)} \ll \bar{\mu}(\partial \bar{u}/\partial y) \quad \text{and} \quad \overline{\rho' u' v'} \ll \bar{\rho}\overline{u'v'}$$

(according to Laufer[18] the density fluctuations have a kinematic rather than a dynamic effect on the turbulence); 4) there is no reaction-generated turbulence[19]; 5) the Lewis number is unity; and 6) Fick's law of binary diffusion is valid.

Following the regular procedure for order-of-magnitude analysis, dominant terms in the time-averaged equations are retained to give the final form of the two-dimensional, steady-state, boundary-layer equations for a reactive turbulent compressible flow (see Ref. 17 for details). These equations for the conservation of mass, momentum, species and enthalpy, and the equation of state are:

$$\frac{\partial}{\partial x}(\bar{\rho}\bar{u}) + \frac{\partial}{\partial y}(\bar{\rho}\bar{v}^\circ) = 0 \tag{1}$$

where $\bar{\rho}\bar{v}^\circ = \bar{\rho}\bar{v} + \overline{\rho' v'}$.

$$\bar{\rho}\bar{u}\frac{\partial \bar{u}}{\partial x} + \bar{\rho}\bar{v}^\circ\frac{\partial \bar{u}}{\partial y} = \frac{\partial}{\partial y}\left[\mu_{\text{eff}}\frac{\partial \bar{u}}{\partial y} - \bar{v}\frac{\mu_t}{C_p\bar{\rho}}\frac{\partial \bar{\rho}}{\partial x}\right] \tag{2}$$

$$\bar{\rho}\bar{u}\frac{\partial \bar{Y}_k}{\partial x} + \bar{\rho}\bar{v}^\circ\frac{\partial \bar{Y}_k}{\partial y} = \frac{\partial}{\partial y}\left[\left(\frac{\mu}{Sc}\right)_{\text{eff}}\frac{\partial \bar{Y}_k}{\partial y}\right] + \bar{\dot{\omega}}_k \tag{3}$$

$$\bar{\rho}\bar{u}\frac{\partial \bar{H}}{\partial x} + \bar{\rho}\bar{v}^\circ\frac{\partial \bar{H}}{\partial y} = \frac{\partial}{\partial y}\left\{\left(\frac{\mu}{Pr}\right)_{\text{eff}}\frac{\partial \bar{H}}{\partial y} + \left[\mu_{\text{eff}} - \left(\frac{\mu}{Pr}\right)_{\text{eff}}\right]\frac{\partial \bar{u}^2/2}{\partial y}\right\} \tag{4}$$

$$\bar{p} = \bar{\rho}R_u\bar{T}/W \tag{5}$$

In arriving at Eqs. (2-4), we have used the following models for various correlations:

1) Reynolds stress $u'v'$ is related to eddy viscosity by the following equation[20]:

$$-\bar{\rho}\overline{u'v'} = \mu_t\frac{\partial \bar{u}}{\partial y} \tag{6}$$

2) Velocity density correlation has been modeled using Boussinesq approximation[20] as:

$$\overline{\rho' u'} = \frac{\mu_t}{C_p\bar{\rho}}\frac{\partial \bar{\rho}}{\partial x} \tag{7}$$

Mass transfer by turbulent diffusion $\overline{(\rho v)' Y_k'}$, and heat transfer by turbulent diffusion $\overline{(\rho v)' h_k'}$, are modeled by using Reynolds' analogy:

$$-\overline{(\rho v)' Y_k'} = \frac{\mu_t}{Sc_t}\frac{\partial \bar{Y}_k}{\partial y}, \quad -\overline{(\rho v)' h_k'} = \frac{\mu_t}{Pr_t}\frac{\partial \bar{h}_k}{\partial y} \tag{8}$$

A two-equation turbulence model,[20] in which the turbulence is assumed to be characterized by its kinetic energy K and its dissipation rate ϵ, has been employed for the closure of the present problem. In addition to the governing equations, Eqs. (1-5), two additional equations for K and ϵ are required. The K equation[17] for a steady, two-dimensional, boundary-layer flow is:

$$\bar{\rho}\bar{u}\frac{\partial K}{\partial x} + \bar{\rho}\bar{v}^\circ\frac{\partial K}{\partial y} = \frac{\partial}{\partial y}\left[\left(\mu + \frac{\mu_t}{C_l}\right)\frac{\partial K}{\partial y}\right] + \mu_t\left[\left(\frac{\partial \bar{u}}{\partial y}\right)^2 - \frac{\bar{v}}{C_p\bar{\rho}}\frac{\partial \bar{\rho}}{\partial x}\frac{\partial \bar{u}}{\partial y}\right] - \bar{\rho}\epsilon \tag{9}$$

The exact form of the ϵ equation for a reacting flow is very difficult to model, because of the appearance of correlations involving fluctuating velocity gradients and density fluctuations. We use the form of ϵ equation as applicable to uniform property flow.[20] However, we modify it by retaining the full expression for production of K, which comprises the second term in square brackets on the right-hand side of Eq. (9). This practice has been followed with good success in reacting flows.[21-24] The ϵ equation[17] for a steady, two-dimensional, boundary-layer flow is:

$$\bar{\rho}\bar{u}\frac{\partial \epsilon}{\partial x} + \bar{\rho}\bar{v}^\circ\frac{\partial \epsilon}{\partial y} = \frac{\partial}{\partial y}\left[\left(\mu + \frac{\mu_t}{C_2}\right)\frac{\partial \epsilon}{\partial y}\right] + C_3\mu_t\left[\left(\frac{\partial \bar{u}}{\partial y}\right)^2 - \frac{\bar{v}}{C_p\bar{\rho}}\frac{\partial \bar{\rho}}{\partial x}\frac{\partial \bar{u}}{\partial y}\right]\frac{\epsilon}{K} - C_4\bar{\rho}\frac{\epsilon^2}{K} \tag{10}$$

The turbulent viscosity μ_t is related to K and ϵ:

$$\mu_t = C_\mu \frac{\bar{\rho} K^2}{\epsilon} \tag{11}$$

where C_μ is a constant. The model of Eq. (11) has been used widely with considerable success.[20-24]

C. Modeling of Gas-Phase Chemical Reactions

The set of equations (1-5) and (9) and (10), with appropriate boundary conditions, can be solved, provided $\dot{\bar{\omega}}_k$ in Eq. (3) is known. When a composite solid propellant burns, solid fuel and oxidizer particles transform into gases. The gases may react in several steps. However, in the present work, the following global single-step-forward chemical reaction is assumed:

$$\nu_F F + \nu_0 0 \rightarrow \nu_P P \tag{12}$$

where O and F represent the oxidizer and the fuel gases, respectively, and P represents the product gases.

The possible expression for the instantaneous global reaction rate is:

$$\dot{\omega}_k = -W_k k_s \Pi_k (\rho Y_k / W_k)^{\nu_k} \tag{13}$$

($k = O, F$, and specific reaction rate constant k_s is given by the Arrhenius law $k_s = A_g \exp[-E_{ag}/R_u T]$). The time averaging of Eq. (13) represents one of the central difficulties of combustion modeling. One can replace the exponential term by its series expansion, thereby introducing correlations such as $\overline{Y_O' Y_F'}$, $\overline{Y_F' T'}$, $\overline{Y_O' T'}$, $\overline{T'^2}$, etc. Additional conservation equations must be solved for these correlations; this procedure, however, reduces the economy significantly and introduces more empiricism into the model.

One other approach, first proposed by Spalding,[25] is the eddy-breakup (EBU) model. In this model it is proposed that the gases in a turbulent flame, at high Reynolds numbers, should be considered as lumps or eddies of unburned and fully burned gas. Spalding assumed that the rate of burning depended upon the rate at which fragments of unburned gas (eddies) were broken into still smaller fragments by the action of turbulence, and that this rate was considered to be proportional to the rate of decay of turbulence energy. Spalding's initial version of the EBU model was based on the mixing-length hypothesis,[25] and Mason and Spalding[24] introduced the EBU model based on the two-equation model of turbulence to solve the problem of confined turbulent flames. The use of the EBU model for diffusion flames has been discussed by Lockwood[26]; Magnussen and Hjertager[27] have used the EBU model for predicting soot formation in a diffusion flame. The EBU concept can be used to model the gas-phase reaction rate for the erosive-burning problem, in which the fuel and oxidizer gases are unmixed as they emerge from the propellant surface. The presence of the high-lateral shear in the boundary layer forms the turbulent eddies. It is reasonable to assume that these eddies engulf fuel and oxidizer gases, giving rise to oxidizer and fuel eddies. Further justification for assuming the existence of fuel eddies comes from the GDF theory,[12] according to which the gaseous fuel emerges as pockets (eddies) from the burning composite propellant surface.

We might then follow the EBU concept and also the arguments of Lockwood[26]: in a diffusion controlled reaction, the rate of consumption of fuel is proportional to the rate of dissipation of the fuel-containing eddies, as characterized by the rate of diminution of the energy of the fluctuations, $g_F \equiv \overline{Y'^2_F}$. This rate can be equated to the rate of supply of energy from the large-scale motion, which can be taken as proportional to the quantity of energy involved and to reciprocal of the eddy time scale characterized by ϵ/K.

$$\dot{\bar{\omega}}_F \propto -\bar{\rho}\sqrt{g_F}(\epsilon/K) \tag{14}$$

Equation (14) can be used, provided g_F is known. The conservation equation for g_F can be solved; however, we have simplified the analysis by assuming the production and dissipation terms of the g_F equation to be dominant. This assumption is particularly good in the near-wall region, which in the current problem is the important region in which most of the chemical reactions take place. Therefore, when equating the production and dissipation terms of the g_F equation (see Ref. 20), we arrive at

$$g_F \propto \frac{\mu_t}{\bar{\rho}} \frac{K}{\epsilon} \left(\frac{\partial \tilde{Y}_F}{\partial y}\right)^2 \tag{15}$$

From Eqs. (11), (14), and (15), we finally get

$$\dot{\bar{\omega}}_F = -C_\omega \bar{\rho} \sqrt{K} \left| \frac{\partial \tilde{Y}_F}{\partial y} \right| \tag{16}$$

where C_ω is a constant. Equation (16) is used along with Eq. (3) to solve species distribution in the gas phase. It should be recognized that the reaction rate represented by Eq. (16) has some limitations. First, it is assumed that the rate of chemical kinetics is very fast, i.e., the reaction is diffusion limited. This assumption is particularly valid for gaseous reactions taking place under high pressures, such as those which exist in actual rocket situations. Second, the use of Eq. (16) is limited to turbulent boundary-layer flows. The primary reason for limiting the current study of erosive burning to turbulent boundary-layer flows is that the flowfield developed over most of the solid propellant grain in a practical rocket motor is turbulent.[16,28] It is believed that the limitations of the current analyses to actual rocket motor situations are far less severe than those analyses which have been limited to laminar boundary-layer flows.[7-9] Further, the application of Eq. (16) to a turbulent boundary-layer flow is more appropriate than the Arrhenius reaction rate law [Eq. (13)], which uses the average temperature and neglects various turbulence correlations. When various turbulence correlations in the Arrhenius reaction rate law are neglected, significant errors may appear in the calculations of reaction rates, as noted by Lockwood.[26]

It may be noted that the species conservation equations are solved for $\tilde{Y}_F$ and $\tilde{Y}_{0F} \equiv [\tilde{Y}_0 - (\nu_0 W_0 / \nu_F W_F)\tilde{Y}_F]$. The choice of the latter variable, with the assumption of Eq. (12), eliminates the nonlinear source term in the equation for this variable. No separate conservation equation is needed for $\tilde{Y}_P$, which is defined as $(1 - \tilde{Y}_0 - \tilde{Y}_F)$.

D. Heat Conduction Equation in the Solid Phase

It is assumed that the heat conduction into the solid propellant is dominant in a direction normal to the burning surface. In a coordinate system attached to the burning surface, the temperature distribution in the solid propellant, at a given x location along the surface, is governed by:

$$\lambda_s \frac{\partial^2 T_p}{\partial y^2} = \rho_s C_s r_b \frac{\partial T_p}{\partial y} \qquad -\infty < y \leq 0 \tag{17}$$

E. Burning Rate Equation

Burning rate of a solid propellant is a function of the surface temperature, and can be expressed by the Arrhenius law of surface pyrolysis:

$$r_b = A_s \exp\left(-\frac{E_{as}}{R_u T_{ps}}\right) \tag{18}$$

It is the surface temperature T_{ps} which provides the link between the burning rate and the gas dynamics. The surface temperature depends on the heat flux from gas to solid phase, and the heat flux is evaluated by solving the gas-phase conservation equations.

F. Boundary Conditions

To complete the formulation of the theoretical model, boundary conditions must be specified at the solid-gas interface as well as at the freestream. The interface mass and energy balance are obtained by considering the flux balance at the solid-gas interface. The mass balance equations can be written as:

$$(\bar{\rho}\bar{v}\tilde{Y}_0)_w - \rho_s r_b Y_{0S} - \left(\bar{\rho}D\frac{\partial \tilde{Y}_0}{\partial y}\right)_w = 0 \tag{19}$$

$$(\bar{\rho}\bar{v}\tilde{Y}_F)_w - \rho_s r_b Y_{FS} - \left(\bar{\rho}D\frac{\partial \tilde{Y}_F}{\partial y}\right)_w = 0 \tag{20}$$

First and second terms of the preceding equations represent, respectively, the component k ($=O$ or F) transported away from the interface by the normal velocity in the gas phase and in the vaporizing solid phase. The third term represents the component k transported from the gas to the solid by diffusion. The energy balance equation is written as:

$$\lambda_s \frac{\partial T_p}{\partial y}\bigg|_w = \lambda \frac{\partial \tilde{T}}{\partial y}\bigg|_w + \rho_s r_b (h_{w-} - h_{w+}) \tag{21}$$

In Eq. (21), the term on the left-hand side represents the net heat flux to the solid propellant; on the right-hand side, the first term represents the heat flux from the gas to solid surface, and the second term represents the net heat release at the surface. Subscripts $(-)$ and $(+)$ represent, respectively, the solid and gas side of the solid-gas interface.

Following Levine and Culick,[29] the net heat release at the surface, per unit mass (equal to the difference between the enthalpies of the gas and solid on their respective sides of the interface), can be expressed as

$$Q_s(T_{ps}) = h_{w+} - h_{w-} = \bar{Q}_s + (C_p - C_s)(T_{ps} - \tilde{T}_{ps}) \tag{22}$$

where $\bar{Q}_s$ is the net surface heat release (negative for exothermic reactions) at a reference surface temperature $\tilde{T}_{ps}$.

By integrating Eq. (17) from $y=-\infty$, where $T_p = T_{pi}$, and $y=0$, where $T_p = T_{ps}$, and using the result along with Eq. (22) in Eq. (21), we find

$$\lambda \frac{\partial T}{\partial y}\bigg|_w = \rho_s r_b [C_p T_{ps} - C_s T_{pi} + \bar{Q}_s + (C_s - C_p)\tilde{T}_{ps}] \tag{23}$$

Boundary conditions for K and ϵ are applied near the wall rather than at the wall. Near a wall, production and dissipation terms in the K equation are equated (a reasonable approximation in this region); therefore,

$$\epsilon = \frac{\mu_t}{\bar{\rho}}\left(\frac{\partial \tilde{u}}{\partial y}\right)^2 \tag{24}$$

Turbulent viscosity μ_t close to the wall is calculated from van Driest's formula.[30]

$$\mu_t = \bar{\rho}(k\mathfrak{D}y)^2 \frac{\partial \tilde{u}}{\partial y} \tag{25}$$

The damping coefficient $\mathfrak{D}$ is given by

$$\mathfrak{D} = 1 - \exp\left(-\frac{y\sqrt{\bar{\rho}\tau}}{A^+\mu}\right) + \exp\left(-\frac{60y}{A^+ R_h}\right) \tag{26}$$

where τ is the local stress, A^+ is a constant, and R_h is the average roughness height. Equation (25) is particularly useful to include the effects of surface roughness on erosive burning. From Eqs. (11), (24), and (25), we find expressions for K and ϵ, as

$$K = \frac{(k\mathfrak{D}y)^2}{\sqrt{C_\mu}}\left(\frac{\partial \tilde{u}}{\partial y}\right)^2 \tag{27}$$

$$\epsilon = (k\mathfrak{D}y)^2 \left|\frac{\partial \tilde{u}}{\partial y}\right|^3 \tag{28}$$

The primary reason for choosing this procedure for the boundary condition of K and ϵ is that the models of various turbulence correlations in the development of K and ϵ equations are inappropriate near a wall. This fact is widely recognized by researchers in the area of the field of turbulence,[20,31] and there is no unique method to avoid this difficulty. Jones and Launder[32] have proposed some modifications in the K and ϵ equations. However, the solutions of modified K and ϵ equations have not been tested widely with experimental data; consequently, the universality of the additional empirical constants introduced in modified K and ϵ equations has not been tested. The near-wall treatment of the K and ϵ equation presented in the current analysis is somewhat similar to that of Chambers and Wilcox.[31] It may be noted that the boundary conditions, Eqs. (27) and (28), give the values of K and ϵ consistent with their distributions in the near-wall region; this becomes apparent when one uses the log law of the wall for velocity in these equations (see Refs. 20 and 31). It may also be noted that Omori,[33] in his calculations of the boundary layer in a rocket motor, has also considered two separate regions of the boundary layer, viz., the viscous sublayer region close to the wall and the wake region. Omori used a K-ℓ model[20] in solving his problem, and in the near-wall region, he used the modified van Driest correlation to specify the eddy viscosity distribution.

Other boundary conditions which are considered in the model are:

At the wall:

$$\tilde{u} = 0, \quad \bar{v} = \rho_s r_b/\rho_w \quad \tilde{T} = \tilde{T}_{p_s} \tag{29}$$

At the freestream:

$$\tilde{u} = U_\infty, \quad \tilde{T} = T_\infty, \quad \tilde{Y}_F = \tilde{Y}_0 = 0, \quad \frac{\partial K}{\partial y} = \frac{\partial \epsilon}{\partial y} = 0 \tag{30}$$

Governing Eqs. (1-5), (9), and (10), with boundary conditions, Eqs. (18-20), (23), and (27-30) complete the theoretical formulation. The system of partial differential equations is parabolic in nature and is solved numerically.

III. Numerical Procedure and Results

A. Numerical Procedure

A number of numerical techniques exist in literature to solve parabolic partial-differential equations. Several researchers[21-24] have used the numerical technique proposed by Patankar and Spalding[34]; the same numerical procedure is followed in this study (see Ref. 17 for details).

About half of the 100 cross-stream intervals employed were distributed within 10% of the boundary-layer thickness, where the dependable variables change rapidly. The forward step size along the x direction is variable and was set at 0.3 times the boundary-layer thickness. Iterations of the boundary-layer solutions were found necessary to obtain a good convergence on the surface temperature. The maximum allowable percentage error in the convergence of the surface temperature was set equal to 0.01.

Table 1 Properties used in theoretical calculations

Property (dimensions)	Propellant type: AP, 75% PBAA/EPON, 25%	AP, 65% Polysulfide, 35%
a (psia/in./s)	230	0
A_s (m/s)	26174 @ $p = 100$ atm	25289@ $p = 100$ atm
A^+ —	26 (Ref. 30)	26
b (psia$^{1/3}$/in./s)	34.5	41.85
c_s (kcal/kg-K)	0.38	0.38
C_p (kcal/kg-K)	0.3	0.3
E_{as} (kcal/mole)	30	30
$\Delta h^\circ_{f,F}$ (kcal/kg)	55.93	−0.42
$\Delta h^\circ_{f,0}$ (kcal/kg)	−942.0	−936.6
$\Delta h^\circ_{f,P}$ (kcal/kg)	−1137.3	−1310.5
k —	0.41	0.41
P_r —	(Svehla's eq.)[35] $\gamma/(1.77\gamma - 0.45)$	same eq.
P_{rt} —	0.9 (Ref. 36)	0.9
$\bar{Q}_s$ (kcal/kg)	−166 (Ref. 12)	−240 (Ref. 35)
Sc —	0.7078	0.7078
Sc_t —	0.9	0.9
Tb_i (K)	298	298
$\bar{T}_{ps}$ (K)	800	800
W_F (kg/kmole)	30	30
W_0 (kg/kmole)	27.893	27.949
W_P (kg/mole)	20.381	25.69
Y_{FS} —	0.25	0.35
Y_{0S} —	0.75	0.65
γ —	1.26	1.26
λ (kcal/m-s-K)	$C_P\mu/Pr$	same eq.
μ_k (kg/m-s)	$8.7\times10^{-8}\sqrt{W_k}\,T^{0.65}$ (Ref. 35)	same eq.
ν_F (kmole)	1	1
ν_0 (kmole)	3.2266	1.9935
ν_p (kmole)	5.888	3.3366
ρ_s (kg/m^3)	1600	1660

Table 2 Constants used in turbulence modeling

Constants	C_1	C_2	C_3	C_4	C_ω	C_μ	C_ρ
Values	1.0	1.3	1.57	2.0	0.18	0.09	1.0
Reference source	20-22	20-22	21	22	24	20-22	21

B. Results and Discussion

Solutions were obtained for two types of composite propellant compositions: 1) ammonium perchlorate (75%) and PBAA/EPON (25%), and 2) ammonium perchlorate (65%) and polysulfide (35%). The various physical properties used in the calculations are given in Table 1, and the values of the constants used in the turbulence modeling are given in Table 2.

It is worthwhile to draw attention to the procedures followed in obtaining some of the properties used in Table 1, especially in the case of those parameters associated with the global single-step-forward reaction. The products generated from the AP primary flame (A/PA flame) due to the chemical reaction between NH_3 and $HClO_4$ are considered to form the equivalent oxidizer gas represented by the symbol $[O]$ in the global reaction. The primary flame is assumed to be collapsed on the propellant surface. The calculations of Steinz et al.[12] demonstrate that in the burning of a composite propellant at normal rocket pressures, the A/P flame is so thin (~1 μm) compared to the oxidizer particle size and the O/F flame thickness that it may be considered to occur at the regressing propellant surface, merely depositing its heat there as gasification takes place. The GDF model[12] considers the effect of A/PA flame on the burning rate of a composite solid propellant when pressure is less than 10 atm. However, under normal rocket-motor pressure ranges (a typical rocket-motor pressure is around 100 atm), the dependence of the burning rate on pressure comes from the O/F diffusion flame of the AP composite propellant. Because the current erosive-burning model is not designed for unrealistically low pressures, the assumption of collapsed A/PA flame is therefore a reasonable one. The exothermic heat of formation of the equivalent oxidizer gas is obtained from the thermochemistry calculation using the CEC72 program.[37] The inputs necessary for this calculation are the heat of formation of the solid AP and the gas pressure. This calculation also gives the average value of the molecular weight of the equivalent oxidizer gas.

It is assumed that the equivalent gaseous fuel, represented by the symbol $[F]$, is formed by the ablation of the solid fuel-binder due to random scission/systematic unzipping of the polymer chain, as discussed in Ref. 12. The heat of formation of the equivalent fuel gas was calculated from the difference between the heat of formation of the solid fuel binder and the heat of decomposition. The heat of formation of the equivalent product gases, represented by symbol $[P]$, is obtained from the overall thermochemistry calculation of AP and fuel-binder combustion. The average molecular weight of the product gases is also determined from this calculation. The stoichiometric coefficient ν_0, ν_F, and ν_p are determined from the mass balance of the global reaction for a given propellant of known initial oxidizer-to-fuel ratio.

The procedure used to calculate the pre-exponential factor in the Arrhenius law of surface pryolysis A_s is as follows: For a particular propellant, the strand burning-rate law is assumed to be known. Using this law, the value of r_{b0} at a pressure of 30 psi can be determined. At this pressure, the measured surface temperature is known[12,38]; therefore, with known r_{b0}, T_{ps}, and E_{as}, Eq. (18) is used to evaluate A_s.

Figure 3 shows the calculated distributions of turbulent kinetic energy, Reynolds stress, and velocity in the chemically reacting turbulent boundary layer considered over the propellant surface. The peak turbulent kinetic energy is located farther from the wall than that in a conventional flat-plate turbulent boundary, due to the strong surface blowing rates caused by the burning of the solid propellant. Calculated

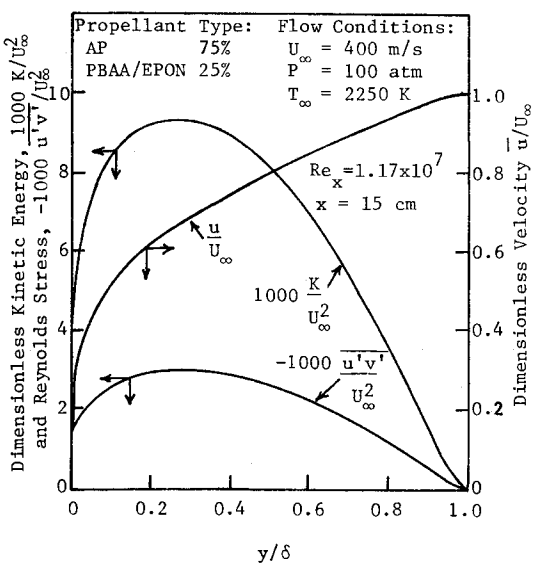

Fig. 3 Calculated distributions of turbulent kinetic energy, Reynolds stress and velocity.

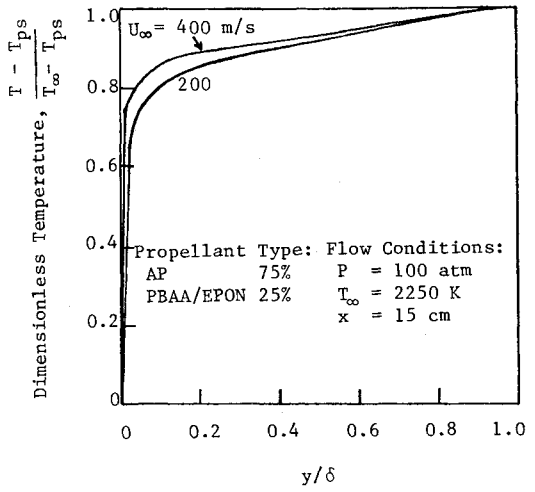

Fig. 4 Calculated temperature distributions for different freestream velocities.

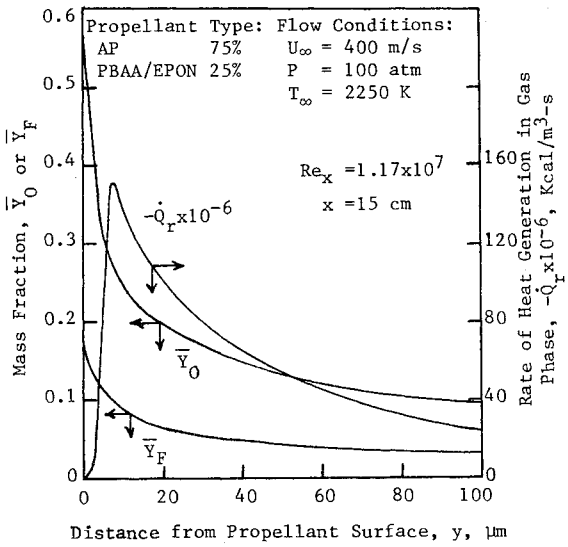

Fig. 5 Calculated distribution of oxidizer and fuel mass fractions, and the rate of heat generation in the gas phase close to the propellant surface.

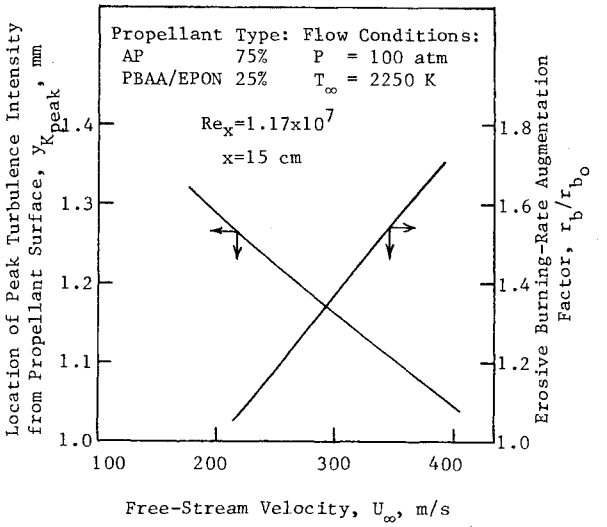

Fig. 6 Effect of freestream velocity on the location of the peak turbulent intensity from propellant surface and the subsequent effect on erosive burning rate.

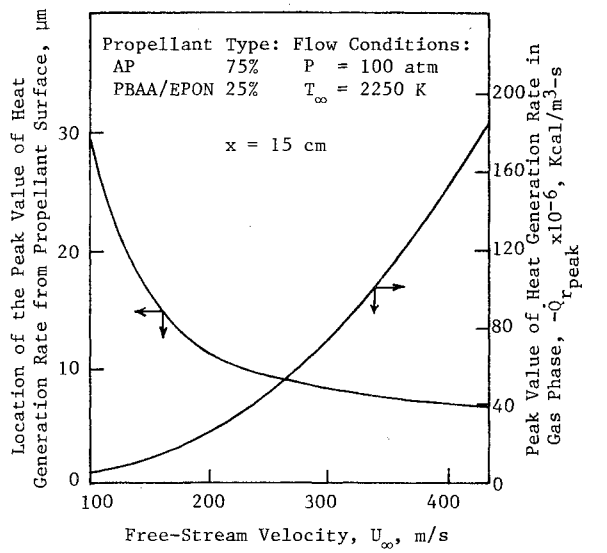

Fig. 7 Effect of freestream velocity on the peak value of heat generation rate in gas phase and its location from propellant surface.

temperature distributions for different freestream velocities are shown in Fig. 4. The temperature rises rapidly from its value at the propellant surface and gradually approaches the freestream gas temperature at the edge of the boundary layer. The rapid rise from the surface is caused by the chemical reactions occurring in the gas-phase region close to the propellant surface as illustrated in Fig. 5, which shows the calculated distribution of the rate of heat generation in the gas phase. Figure 5 also shows the distributions of the oxidizer and fuel mass fractions which drop to very small values in a region close to the propellant surface, due to the higher rate of reaction of this region.

The temperature gradient becomes steeper (higher gas-to-solid heat flux) at the surface as the freestream velocity increases (see Fig. 4). This is expected because the higher the level of turbulent intensity, the higher the chemical reactions in the gas phase. This effect can be seen from the results plotted in Figs. 6 and 7. The results of Fig. 6 show that the increase in freestream velocity brings the location of the peak turbulent intensity closer to the propellant surface. This has a significant effect on the flowfield near the propellant surface. The closeness of the peak turbulence intensity to propellant surface means that the turbulent eddies with high frequencies also come closer to the propellant surface. This causes an increase in the mixing rate of oxidizer and fuel species, therefore increasing the gas-phase reaction rate and bringing it closer to the propellant surface. The results plotted in Fig. 7 show that the peak value of the heat generation rate in the gas phase, due to chemical reactions, increases with increasing velocity, and the location of this peak comes closer to the propellant surface. Therefore, the increased heat flux eventually increases the erosive burning augmentation factor (r_b/r_{b0}), as shown in Fig. 6.

It may be noted that for any U_∞, the location of the peak value of K (Fig. 6) is farther away from the propellant surface than the location of the maximum value of $\dot{Q}_r$ (Fig. 7). This, however, does not mean that the turbulence has negligible influence in the gaseous reactions in a region where the reaction rate is maximum (corresponding to maximum $\dot{Q}_r$). For example, present calculations (for $U_\infty = 400$ m/s) show that μ_t in this region is more than 10 times the value of μ. Therefore, there is a strong effect of turbulence in this region, even though the peak value of K is away from this region. It is clear from Eq. (16) that the reaction rate is influenced not only by the level of K, but also by the gradient $\tilde{Y}_F$ which is steeper near the propellant surface. Thus the maximum

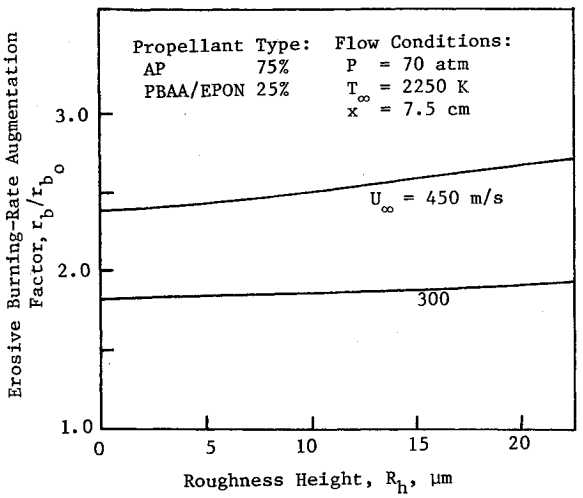

Fig. 8 Computed erosive burning rate augmentation factor showing the effect of propellant-surface roughness height at different freestream velocities.

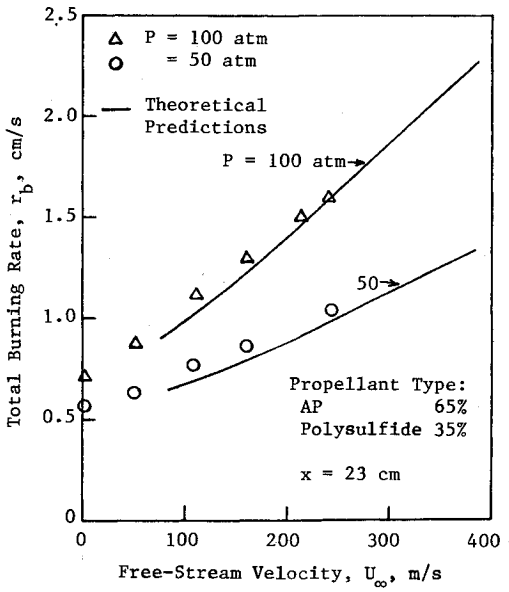

Fig. 9 Comparison of the predicted erosive burning rates with the experimental data of Marklund and Lake.[39]

reaction rate region is much closer to the propellant surface than the location of peak turbulence intensity.

The turbulent nature of the flowfield over the propellant surface contributes in two important ways to the erosive burning situation. First, it enhances the diffusional mixing of the fuel and oxidizer gases, bringing the gas-phase reaction zone and the heat-release zone closer to the propellant surface as the freestream velocity increases. Second, the rate of heat transfer to the propellant surface is increased because the turbulence increases transport coefficients of the gas phase. The overall effect of turbulence, therefore, is to enhance heat feedback which, in turn, increases the burning rate of a propellant as shown in Fig. 6.

Figure 8 demonstrates the effect of surface roughness on the augmentation factor for different freestream velocities. As the roughness height increases, the augmentation factor also increases. This is to be expected since roughness aids the fuel and oxidizer mixing process, because of increased turbulent activity closer to the propellant surface. However, the effect of roughness diminishes for lower freestream velocities. This is because the viscous sublayer thickness increases at low velocities, submerging the roughness elements in the sublayer

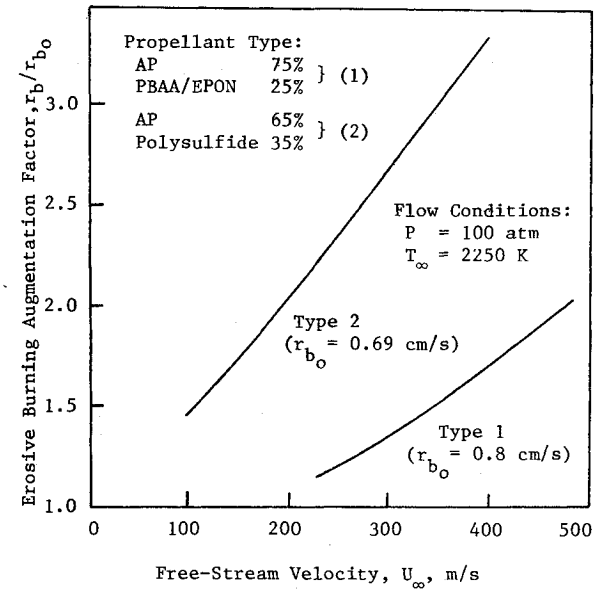

Fig. 10 Effect of normal burning rate on the erosive burning rate augmentation factor.

and, therefore, lessening their effect on the erosive burning process.

Figure 9 shows the predicted erosive burning rates for AP/polysulfide propellant, and the results are compared with the experimental data of Marklund and Lake.[39] The results were computed at the same Reynolds number as in the experiments described in Ref. 39. The effect of freestream velocity on total burning rate is compared at two pressures of 100 and 50 atms. Total burning rate increases with an increase in either pressure or velocity. The figure indicates that the agreement between the theoretical and experimental results is very close. It may be pointed out that the present computations are not carried out for very low freestream velocities (<80 m/s), because then the ratio $\rho_s r_b/\rho_\infty U_\infty$ is no longer small and the boundary-layer approximation used in the current model will be violated.

Figure 10 shows the effect of normal burning rate on the erosive burning rate augmentation factor. The AP/polysulfide propellant (type 2), with a lower value of normal burning rate, is found to be more sensitive to erosive burning than that of the propellant (type 1) which has a higher value of normal burning rate. This observation is consistent with the experimental observation of Marklund and Lake.[39]

IV. Summary and Conclusions

1) The erosive burning problem of composite solid propellants has been modeled by considering a two-dimensional, chemically reacting, turbulent boundary layer over a propellant surface. The theoretical model has been solved numerically, and the predicted erosive burning rates showed a close agreement with the experimental data of Marklund and Lake.[39]

2) The predicted results also show that propellants with lower normal burning rates are more sensitive to erosive burning than those with higher normal burning rates; and, the surface roughness of a propellant augments the erosive burning rate of a composite solid propellant.

3) The basic mechanism for the erosive burning effect is believed to be the increased heat feedback to propellant surface introduced by the increase in transport coefficients, and the turbulence-enhanced mixing and reaction of the oxidizer and fuel gases. In addition, the increase in freestream gas velocity brings the location of the peak turbulence intensity and the reaction zone closer to the propellant surface. Thus, more heat is released near the surface, thereby in-

creasing the heat feedback to the propellant surface and the burning rate of a solid propellant.

Acknowledgment

A part of this work was performed under the sponsorship of the Air Force Office of Scientific Research, (AFOSR), Bolling Air Force Base, Washington, D.C., under Contract No. AFOSR-76-2914. Currently, the work is being done under a subcontract from the Atlantic Research Corporation, which is the prime contractor for AFOSR under the management of R. F. Sperlein, Contract No. F49620-78-C-0016.

References

[1] Kuo, K. K. and Razdan, M. K., "Review of Erosive Burning of Solid Propellants," *12th JANNAF Combustion Meeting*, CPIA Publication 273, Vol. II, 1975, pp. 323-338.

[2] King, M. K., "Review of Erosive Burning Models," *JANNAF Workshop on Erosive Burning/Velocity Coupling*, Lancaster, Calif., March 1977.

[3] Lenoir, J. M. and Robillard, G., "A Mathematical Method To Predict the Effects of Erosive Burning in Solid-Propellant Rockets," *Sixth Symposium (International) on Combustion*, Reinhold, New York, 1957, pp. 663-667.

[4] Vandenkerckhove, J. A., "Erosive Burning of a Colloidal Solid Propellant," *Jet Propulsion*, Vol. 28, Sept. 1958, pp. 599-603.

[5] King, M. K., "An Analytical and Experimental Study of the Erosive Burning of Composite Propellants," AFOSR-TR-78-0060, Final Report to U.S. Air Force Office of Scientific Research, Nov. 1977.

[6] Corner, J., *Theory of Interior Ballistics of Guns*, John Wiley and Sons, New York, 1950, pp. 73-81.

[7] Tsuji, H., "An Aerothermochemical Analysis of Erosive Burning of Solid Propellant," *Ninth Symposium (International) on Combustion*, Williams & Wilkins, Baltimore, Md., 1963, pp. 384-393.

[8] Razdan, M. K. "Theoretical Studies on the Erosive Burning of Double-Base Solid Propellants," Master of Technology Thesis, Indian Institute of Technology, Kanpur (1974).

[9] Schuyler, F. L. and Torda, T. P., "An Aerothermochemical Analysis of Solid Propellant Combustion," *AIAA Journal*, Vol. 4, Dec. 1966, pp. 2171-2177.

[10] Lengelle, G., "Model Describing the Erosive Combustion and Velocity Response of Composite Propellants," *AIAA Journal*, Vol. 13, March 1975, pp. 315-322.

[11] Beddini, R., "Reacting Turbulent Boundary-Layer Approach to Solid Propellant Erosive Burning," *AIAA Journal*, Vol. 16, Sept. 1978, pp. 898-905.

[12] Steinz, J. A., Stang, P. L., and Summerfield, M., "The Burning Mechanism of Ammonium Perchlorate-Based Composite Solid Propellants," AIAA Paper 68-658, 1968.

[13] Beckstead, M. W., Derr, R. L., and Price, C. F., "A Model of Composite Solid Propellant Combustion Based on Multiple Flames," *AIAA Journal*, Vol. 8, Dec. 1970, pp. 2200-2207.

[14] Squire, L. C., "The Constant Property Turbulent Boundary Layer with Injection; A Reanalysis of Some Experimental Results," *International Journal of Heat Mass Transfer*, Vol. 13, May 1970, pp. 939-942.

[15] Mickley, H. S. and Davis, R. S., "Momentum Transfer for Flow over a Flat Plate with Blowing," NACA TN 4017, Nov. 1957.

[16] Makunda, H. S., "A Comprehensive Theory of Erosive Burning in Solid Rocket Propellants," *Combustion Science and Technology*, Vol. 18, Nos., 3 and 4, 1978, pp. 105-118.

[17] Razdan, M. K. and Kuo, K. K., "Erosive Burning Studies of Composite Solid Propellants by the Reacting Turbulent Boundary-Layer Approach, AFOSR-TR-78-0035, Tech. Rept. to U.S. Air Force Office of Scientific Research, Nov. 1977.

[18] Laufer, J., "Thought on Compressible Turbulent Boundary Layers," NASA SP-216, Dec. 1968.

[19] Kulgein, N. G., "Transport Processess in a Compressible Turbulent Boundary Layer," *Journal of Fluid Mechanics*, Vol. 12, March 1962, pp. 417-437.

[20] Launder, B. E. and Spalding, D. B., *Mathematical Models of Turbulence*, Academic Press, New York, 1972, p. 9.

[21] Lockwood, F. C. and Naguib, A. S., "The Prediction of the Fluctuations in the Properties of Free, Round-Jet, Turbulent, Diffusion Flames," *Combustion and Flame*, Vol. 24, No. 1, 1975, pp. 109-124.

[22] Gosman, A. D., Lockwood, F. C., and Syed, S. A., "Prediction of a Horizontal Free Turbulent Diffusion Flame," *Sixteenth Symposium (International) on Combustion*, Combustion Institute, 1976, pp. 1543-1555.

[23] Elghobashi, S. E. and Pun, W. M., "A Theoretical and Experimental Study of Turbulent Diffusion Flames in Cylindrical Furnaces," *Fifteenth Symposium (International) on Combustion*, Combustion Institute, 1974, pp. 1353-1365.

[24] Mason, H. B. and Spalding, D. B., "Prediction of Reaction Rates in Turbulent Pre-Mixed Boundary Layer Flows," *Combustion Institute, First European Symposium*, 1973, pp. 601-606.

[25] Spalding, D. B., "Mixing and Chemical Reaction in Steady Confined Turbulent Flames," *Thirteenth Symposium (International) on Combustion*, Combustion Institute, 1971, pp. 649-657.

[26] Lockwood, F. C., "The Modeling of Turbulent Premixed and Diffusion Combustion in the Computation of Engineering Flows," *Combustion and Flame*, Vol. 29, No. 2, 1977, pp. 111-122.

[27] Magnussen, B. F. and Hjertager, B. H., "On Prediction of Soot Formation and Combustion in Turbulent Flames with Special Reference to a Free-Jet C_2H_2 Diffusion Flame," *Combustion Institute, 2nd European Symposium*, Vol. 1, 1975, pp. 385-390.

[28] Williams, F. A., Berrieré, M., and Haung, N. C., "Fundamental Aspects of Solid Propellant Rockets," AGARDograph-116, Technivision, 1969, p. 438.

[29] Levine, J. N. and Culick, F.E.C., "Nonlinear Analysis of Solid Rocket Combustion Instability," AFRPL-TR-74-45 Final Rept., Vol. I, 1974.

[30] van Driest, E. R., "On Turbulent Flow Near a Wall," *Journal of the Aeronautical Sciences*, Vol. 23, Nov. 1956, pp. 1007-1011.

[31] Chambers, T. L. and Wilcox, D. C., "Critical Examination of Two-Equation Turbulence Closure Models for Boundary Layers," *AIAA Journal*, Vol. 15, June 1977, pp. 821-828.

[32] Jones, W. P. and Launder, B. E., "The Calculation of Low-Reynolds-Number Phenomena with a Two-Equation Model of Turbulence," *International Journal of Heat Mass Transfer*, Vol. 16, June 1973, pp. 1119-1129.

[33] Omori, S., "Eddy Viscosity Calculation Along the Chemical Rocket Thrust Chamber Wall Using Turbulent Kinetic Energy," *Combustion Science and Technology*, Vol. 7, No. 6, 1973, pp. 229-240.

[34] Patankar, S. V. and Spalding, D. B., *Heat and Mass Transfer in Boundary Layers*, Inter-text Books, London, 1970.

[35] Peretz, A., Kuo, K. K., Caveny, L. H., and Summerfield, M., "Starting Transient of Solid Propellant Rocket Motors with High Internal Gas Velocities," *AIAA Journal*, Vol. 11, Dec. 1973, pp. 1719-1727.

[36] Kays, W. M., "Heat Transfer to the Transpired Turbulent Boundary Layer," *International Journal of Heat Mass Transfer*, Vol. 15, May 1972, pp. 1023-1044.

[37] Gordon, S. and McBride, B. J., "Computer Program for Calculation of Chemical Equilibrium Compositions, Rocket Performance, Incident and Reflected Shocks, and Chapman-Jouguet Detonations," NASA SP-273, 1971.

[38] Sabadell, A. J., Wenograd, J., and Summerfield, M., "Measurement of Temperature Profiles Through Solid Propellant Flames Using Fine Thermocouples," *AIAA Journal*, Vol. 3, Sept. 1965, pp. 1580-1584.

[39] Marklund, T. and Lake, A., "Experimental Investigation of Propellant Erosion," *ARS Journal*, Vol. 3, Feb. 1960, pp. 173-178.